

Energy Photovoltaics, Inc.
276 Bakers Basin Road
Lawrenceville, NJ 08648

July 18, 2006

Dr. Harin Ullal, Technical Monitor
National Renewable Energy Laboratory
1617 Cole Boulevard
Golden, CO 80401

Dear Harin,

This is the first quarterly report for Phase II of EPV's cost-shared subcontract ZXL-5-44205-05 "Uniform, High Efficiency, Hybrid CIGS Processing with Application to Novel Device Structures" awarded under the Thin Film Photovoltaics Partnership Program. The nominal period covered by the report is 03/18/06 – 06/17/06.

The core CIGS group consists of Dr. Alan Delahoy, Dr. Baosheng Sang, Dr. Masud Akhtar, Ramesh Govindarajan, and Renata Saramak. Dr. Sheyu Guo is assisting with development of front and back contact materials for CIGS devices.

The following sections summarize our main activities in this quarter and present some relevant news items:

- 1) Small area devices in R&D system Hercules;
- 2) Large area modules in Zeus;
- 3) Exploring new buffer layers;
- 4) Optical films produced by RE-HCS;
- 5) Relevant news items.

1) Small area devices in R&D system Hercules

In this quarter, we continued to explore deposition of CIGS of submicron thickness focusing on thicknesses around 0.5 μm . The CIGS films were prepared using the simplified hybrid process. Table I summarizes the performance of our best cells at various CIGS thicknesses from 1.3 to 0.5 μm . All devices had the same baseline structure of SLG/Mo/CIGS/CdS/i-ZnO/ZnO:Al. It is observed that device efficiency progressively drops from 13% to 10% as CIGS thickness decreases from 1.3 μm to 0.5 μm . Figure 1a shows the variation of efficiency versus thickness for these cells and some others. Figure 1b shows the variation of V_{oc} , J_{sc} and FF for the set of cells in Table I. Although J_{sc} falls off as expected, V_{oc} and FF also decrease when the CIGS is thinned down to 0.5 μm . For current, one cause is insufficient optical absorption of long-wavelength incident photons. This can be seen in the QE data shown in Fig. 2. However, this figure also reveals a drop in the peak QE at a thickness of 0.5 μm . The lower V_{oc} and FF might result from back surface recombination, but this is not clear. An additional, but trivial, reason could be shunting that might result from the use of an indium dot electrode that is pressed onto the n-ZnO.

Table I. Device performance at various CIGS thicknesses

Run	Thickness (μm)	Ga/(In+Ga)	V_{oc} (mV)	J_{sc} (mA/cm^2)	FF (%)	Eff (%)
H080205-4	1.30	0.32	587	33.2	68.5	13.4
H121405-2	1.13	0.37	622	29.4	72.7	13.3
H060105-6	1.00	0.33	626	29.2	72.3	13.2
H052405-6	0.92	0.38	638	28.7	70.0	12.8
H052305-5	0.85	0.36	608	27.9	70.5	12.0
H052005-1	0.82	0.32	605	29.4	67.9	12.1
H071205-4	0.74	0.29	590	29.1	70.5	12.1
H040406-5	0.52	0.35	562	27.1	65.4	10.0
H032206-5	0.48	0.31	532	26.6	65.6	9.3
H032906-5	0.47	0.30	576	26.8	64.2	9.9

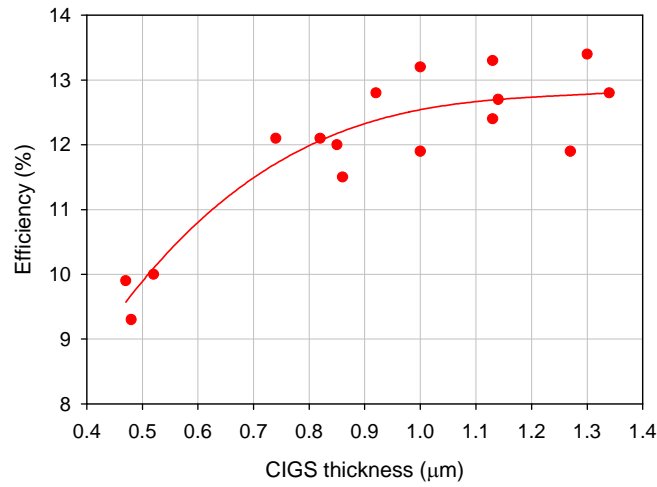


Fig. 1a. Cell efficiency vs CIGS thickness

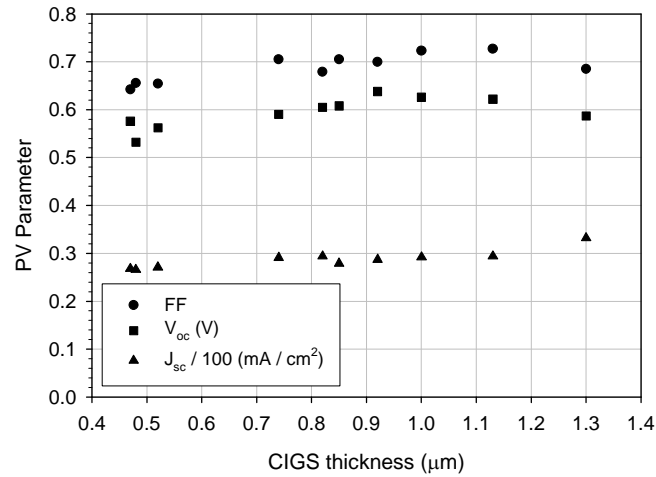


Fig. 1b. Other cell PV parameters vs CIGS thickness

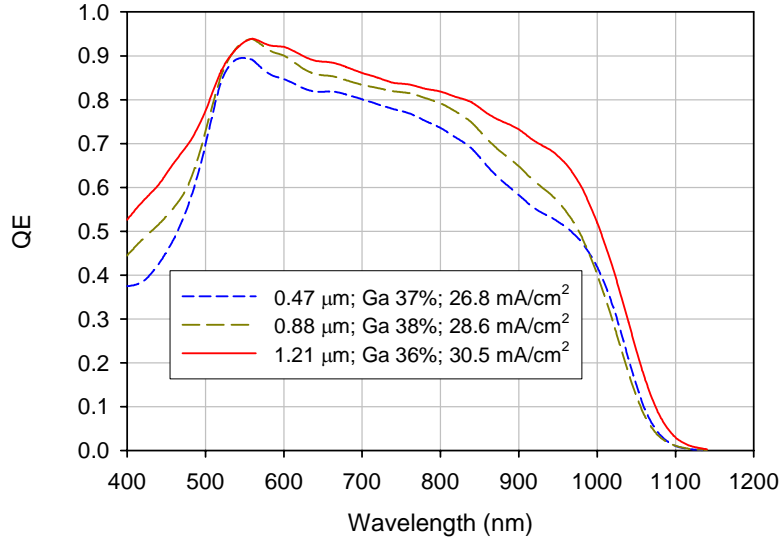


Fig. 2. External QE of cells with different CIGS thickness

With a view to re-gaining the lost current, application of a highly reflective back contact layer such as TiN is underway [1]. We have also started to prepare prototype light-trapping structures using texturing. The first device of this type that was made was 0.47 μm in thickness and employed both texturing and a Mo / TiN back contact. Its performance was disappointing, the PV parameters being 405 mV, 24.4 mA/cm^2 , FF 47.8%, Eff. 4.7%.

In order to understand our simplified hybrid process and further improve our CIGS film deposition and device performance, CIGS films were sent to NREL for compositional analyses using AES (we acknowledge Craig Perkins and Sally Asher for the measurements). Figure 3 shows the compositional profile (left), and calculated Ga/(In+Ga), Cu/(In+Ga) distribution (right) for a CIGS film. This film (H120605) is 1.1 μm thick and yielded device efficiencies up to 14% as reported previously [1]. The Ga/(Ga+In) distribution is fairly uniform although there is a small and gradual increase of Ga/(Ga+In) throughout the CIGS layer in the direction of the Mo layer which is desirable for enhancing collection of carriers generated at the rear of the cell i.e. near the CIGS/Mo interface. It also appears that Cu/(In+Ga) declines significantly from 0.8 to 0.4 in the top 0.2 μm of the CIGS, and that the Se content increases slightly towards the top surface. We do not know yet if this composition change reflects the existence of a different phase, e.g. $\text{Cu}(\text{InGa})_3\text{Se}_5$, which is an ordered vacancy compound with a band gap higher than that of $\text{Cu}(\text{InGa})\text{Se}_2$. Additional analyses, such as XRD measurements, would be needed to investigate this.

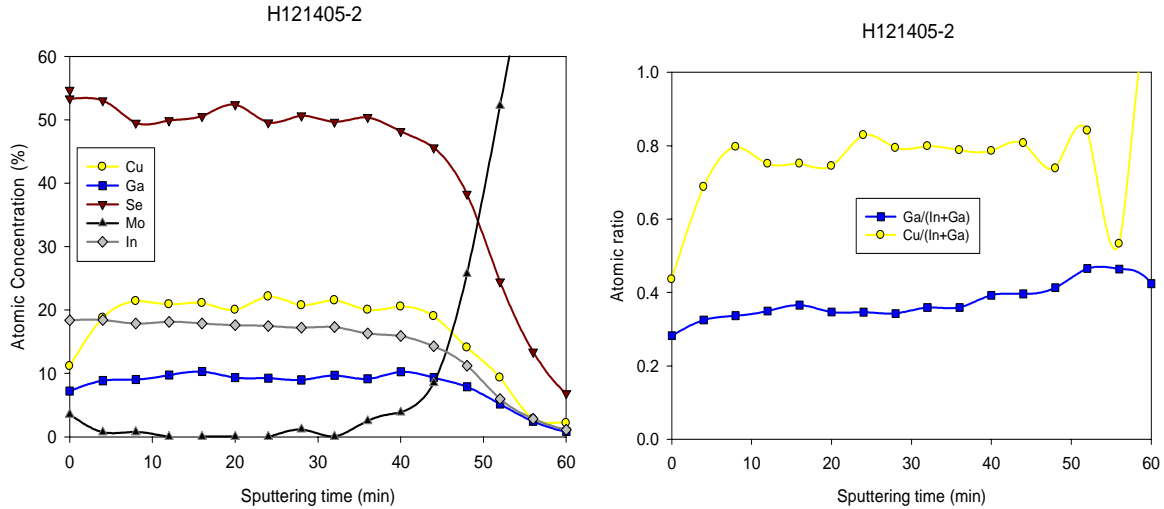


Fig. 3. Atomic concentration profiles of CIGS from AES measurement

We also noticed some nodules and places where these nodules had apparently pulled out of the film, as shown in Fig. 4.

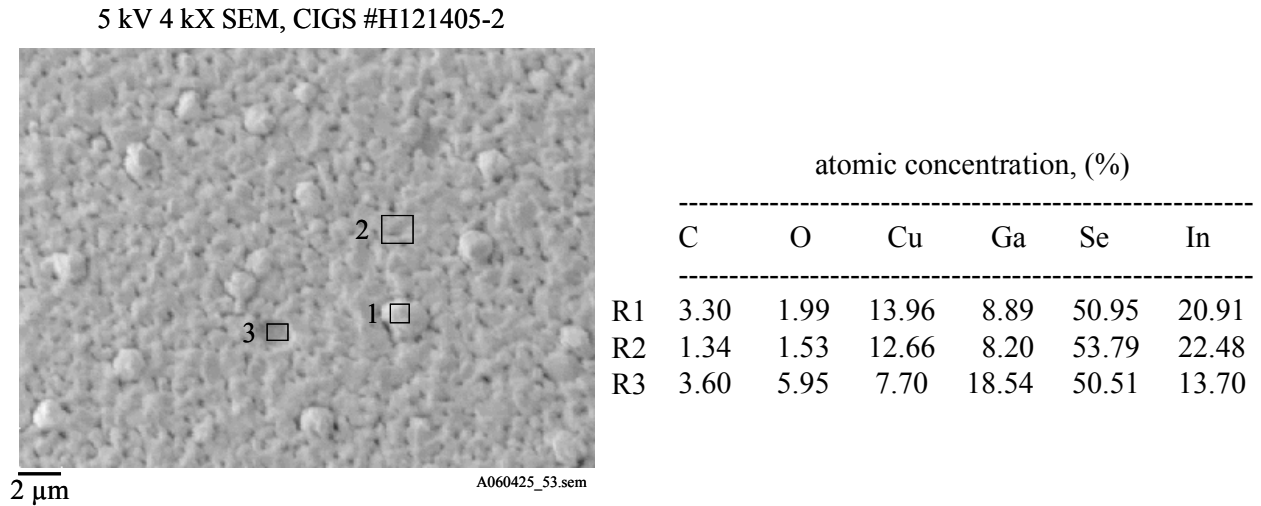


Fig. 4. SEM image and composition at different film areas (R1: on nodule, R2: on normal part of film, R3: in crater)

It is observed that there is a compositional difference among these areas (as given in the table). It needs to be investigated if and how these nodules affect CIGS device performance. On the other hand, their elimination may offer the opportunity to further improve our CIGS film quality and device performance. We intend to change both the metal fluxes to reduce deposition rate during the last stage and the substrate temperature ramp-down profile after deposition to see if nodule formation can be avoided.

2) Large area CIGS modules

We re-started our full size module production in this quarter following the success of transplanting the Simplified Hybrid Process from the R&D Hercules system to the large area Zeus system as described in the recent annual report for Phase I of the subcontract [1].

A baseline procedure for CIGS module fabrication had already been established with our original hybrid process [2], but we found that some adjustments were necessary (e.g. post laser scribing treatment) for the new hybrid process. Table II lists the performance of the initial test modules. All full size modules generate a power of around 20 W, which is a very encouraging start. Efficiency is still slightly lower than that of our best modules made using the original hybrid process; figures for the best of the latter modules are shown in italics in the last line of the table. It should be pointed out that the CIGS film thickness for modules produced using the simplified hybrid process is about 1.3 μm while the CIGS thickness of Z1668 is 2.5 μm . This contributes to the lower J_{sc} of the former set of modules. While V_{oc} is comparable, the lower FF recently observed is believed to result mostly from CIGS film quality but also from other factors such as ZnO/Mo contact resistance. We will continue to focus on improving both the quality and uniformity of the CIGS film, adjusting ZnO deposition procedure to reduce ZnO/Mo contact resistance, and controlling scribe quality.

Table II. Performance of first large area modules made using the simplified hybrid process

ID	V_{oc} (V)	I_{sc} * (A)	FF (%)	Power (W)	Efficiency (%)	# seg- ments	$V_{\text{oc}}/\text{cell}$ (mV)	J_{sc} (mA/cm^2)	Ap. area (cm^2)
Z1803	34.5	1.14	46.5	19.3	5.6	71	486	23.3	3462
Z1804	39.0	1.02	48.0	19.0	5.6	71	548	21.1	3414
Z1805	37.9	1.14	51.7	22.4	6.2	71	533	22.4	3612
Z1806	38.2	1.23	53.0	24.9	6.7	71	537	23.4	3732
Z1807	34.7	1.18	51.8	21.1	6.0	71	489	23.6	3533
<i>Z1668</i>	<i>38.5</i>	<i>1.20</i>	<i>56.4</i>	<i>26.0</i>	<i>7.5</i>	<i>71</i>	<i>542</i>	<i>24.7</i>	<i>3450</i>

* Outdoor measurement normalized to one sun

3) Exploring new buffer layers

We studied the effect of addition of iso-propyl alcohol in the chemical bath deposition of the buffer films CdS, ZnS, and (CdZn)S. We tried to follow the work of Bhattacharya et al. [3]. It was reported by Bhattacharya during the 2006 National CIS R&D Team Meeting that the i-ZnO layer could be omitted by use of a Cd:ZnS(O,OH) buffer layer. If this result could be repeatably achieved in the industry, it can eliminate the i-ZnO formation step before the P2 scribe, yielding a benefit in module production. Although a very high ammonia concentration of 9M was used in Bhattacharya's work, we employed the usual ammonia concentration of about 2.5M and set the bath temperature in the range of 66-70°C. The initial work did not clearly indicate the success of Zn incorporation in the buffer layer. We will continue to explore the process.

4) Optical films produced by RE-HCS

Reactive-environment hollow cathode sputtering has been used to prepare TiN for use as a back contact material and ZnO:Al as a top TCO [4]. The spectral reflectance of TiN is shown in Fig. 5 and is compared to that of Mo. TiN exhibits a higher reflectivity in the near IR.

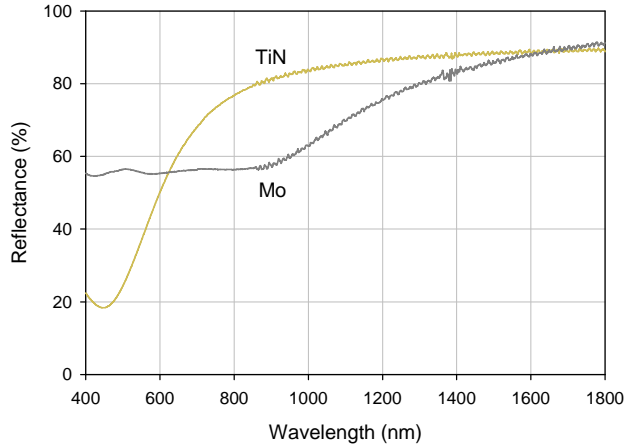


Fig. 5. Spectral reflectance of TiN and Mo

With the goal of developing TCOs by a low-cost process with intrinsic process stability, we have applied the RE-HCS method to the production of doped ZnO and In_2O_3 layers using metallic Zn and In targets. Here we report results for ZnO:Al obtained by sputtering a separate doping target (an Al bar) located in the Ar flow and near the entrance of the cathode cavity. Fig. 6 shows the dependence of ZnO:Al resistivity ρ on Al content. With an RF bias of -30 V, $\rho = 3.6 \times 10^{-4} \Omega \text{ cm}$ was reached.

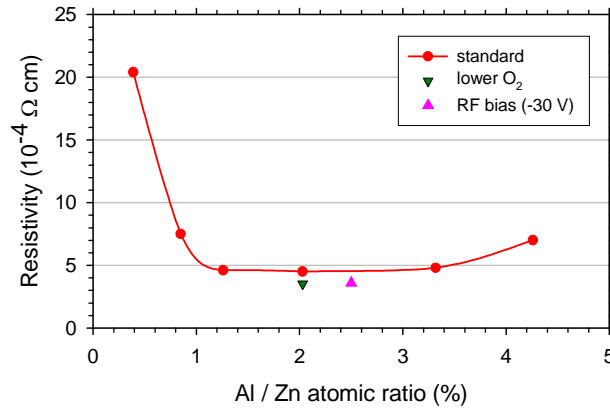


Fig. 6. Resistivity of ZnO:Al versus Al / Zn ratio

We have explored the use of RE-HCS to produce the ZnO:Al top TCO in CIGS devices, and compare these results with those obtained with conventional RF magnetron ZnO:Al (see Table III). The RE-HCS process for ZnO:Al yields at least equivalent devices and can be adopted for routine device fabrication.

Table III. Comparison of CIGS cells produced with RE-HCS and RF magnetron sputtered ZnO TCOs

Cell type	ZnO method	V _{oc} (mV)	J _{sc} (mA/cm ²)	FF (%)	Eff. (%)
Mo/CIGS/CdS/i-ZnO/n ⁺ -ZnO	RE-HCS	577	29.4	66.1	11.2
Mo/CIGS/CdS/i-ZnO/n ⁺ -ZnO	RF magnetron	533	29.7	70.3	11.1

5) Relevant news items

- Dr. Alan Delahoy presented a talk entitled “Uniform, High Efficiency, Hybrid CIGS Processing with Application to Novel Device Structures” at National CIS R&D Team Meeting in Golden, CO on April 6, 2006.
- Dr. Alan Delahoy presented an invited paper entitled “Reactive-Environment Hollow Cathode Sputtering: Compound Film Production, and Application to Thin Film Photovoltaics” at the 4th World Conference on Photovoltaic Energy Conversion in Hawaii on May 9, 2006.
- A significant financial restructuring of EPV was consummated on July 17, 2006 resulting in EPV having a financial and ownership structure that sets the stage for future growth.

References:

- [1] A.E. Delahoy, L. Chen, and B. Sang, “Uniform, High Efficiency, Hybrid CIGS Process with Application to Novel Device Structures”, Phase I Annual Technical Report, NREL/SR-520-40145 (2006).
- [2] A.E. Delahoy and L. Chen, “Advanced CIGS Photovoltaic Technology”, Phase II Annual Technical Report, NREL/SR-520-35922 (2004).
- [3] Bhattacharya et al., “Jpn. J. Appl. Phys. 2004, 43, L1475-76.
- [4] A.E. Delahoy, S. Guo, J. Cambridge, R. Lyndall, J.A. Anna Selvan, A. Patel, A. Foustotchenko, and B. Sang, presented at the 4th World Conference on Photovoltaic Energy Conversion, Waikoloa, Hawaii, 2006.

Sincerely,



Alan E. Delahoy
Principal Investigator



Baosheng Sang
Scientist